JOURNAL OF COMPUTATIONAL PHYSICS **146,** 691–706 (1998)
ARTICLE NO. CP986079

# A Quasi-Two-Dimensional Benchmark Problem for Low Mach Number Compressible Codes

Ananias G. Tomboulides*,[1] and Steven A. Orszag†,[2]

*Department of Aerospace and Mechanical Engineering, Boston University, 110 Cummington St., Boston, Massachusetts 02215; †Department of Mathematics, Yale University, New Haven, Connecticut 06511
E-mail: at@omega.bu.edu

Received January 12, 1998; revised July 30, 1998

A quasi-two-dimensional model problem is presented, which can be used as a benchmark problem for verification of numerical methods for the solution of the low Mach number compressible reactive flow equations. A recently developed high order splitting method for this type of problem is presented and analyzed, and the behavior of the numerical errors is assessed and compared to asymptotic estimates. It is found that the behavior of splitting errors is predicted well by the asymptotic estimates and that these errors are always smaller than the formal truncation order of the integrating scheme. 

*Key Words:* compressible reactive flows; splitting errors; time stepping; backward differentiation; combustion.

## 1. INTRODUCTION

In the numerical solution of low speed compressible reacting flows involved in combustion problems, the existence of high frequency acoustic waves places a severe restriction on time steps. In order to deal with this difficulty, one can decouple acoustic waves from the equations (when such waves are not of interest) using regular perturbation theory, and obtain a set of approximate equations which are free of acoustic wave interactions [1–3]. In this set of equations, the pressure appears at leading order in the energy and state equations ("thermodynamic pressure") and at first order in the momentum equation ("hydrodynamic pressure"). Several approaches have been used for the integration of the conservation equations of low speed combustion and a fairly comprehensive review of earlier works is given in [4]. Recently, two-dimensional simulations of reactive flows with both simple and detailed chemistry and transport have been reported in [5–9], and in references therein.

[1] Corresponding author.

[2] Hamrick Professor Emeritus, Princeton University.



0021-9991/98 $25.00

Although several numerical approaches have been employed for the simulation of low speed compressible reacting flows, one can find very few cases where the overall convergence rate, local error behavior, and/or stability properties of these approaches have been analyzed in detail. Using one-dimensional benchmark problems to verify numerical methods for complex two- and three-dimensional reactive flow problems cannot provide answers to the questions above. More complex 2D benchmark problems are needed for this purpose, and these are not readily available in the literature. Verifying the order of accuracy and stability properties of fully explicit time integration methods [10, 11] is fairly straightforward; however, these schemes suffer from severe time-stepping restrictions. The restrictions become even more pronounced when solving the full set of conservation equations at very low Mach numbers. This is why many approaches employed today perform some type of time-splitting in the solution procedure [12], where some of the terms in the equations are treated implicitly and others explicitly (most commonly the nonlinear convective terms), resulting in less severe time-stepping restrictions. In addition, pressure correction or projection methods, [7–9], are used to incorporate the effects of the pressure in low speed compressible flows; in many cases this leads to coupled iterative solution procedures. To analyze the error behavior of these types of methods is not straightforward. For example, second-order finite differences are very commonly used, in space and time, for the simulation of 2- and 3D reactive flow phenomena. Unless fully explicit schemes are used, the use of operator splitting in the solution procedure reduces the overall order of accuracy in time to first, or at best to between first and second order. The overall result is similar when using other higher order methods in time. It is known [13] that operator splitting, or fractional stepping, needs to be carefully applied in order to maintain globally the high-order accuracy of the schemes used. This issue is the main focus of the current investigation.

Here we present and analyze a new numerical approach, originally reported in [14], for the integration of the governing equations of low Mach number compressible flow. To analyze this approach, we use an integrated asymptotic and numerical analysis of a quasi-two-dimensional model problem. Here, quasi-two-dimensional denotes a two-dimensional problem where one of the dimensions (in this case $y$) is of infinite extent. In this way, periodicity can be assumed in this direction, with specified wavenumber, and a normal mode analysis using Fourier series can be performed. In order to facilitate the presentation, several assumptions will be made. As a first approximation, detailed transport processes are neglected and only one-step overall reaction mechanisms are considered. In fact, for the model problem the species conservation equations are dropped and only the energy, together with the momentum and mass conservation equations, is used. In addition, all dynamic transport coefficients (in particular, the dynamic viscosity and heat transport coefficient $\mu$, $\lambda$, respectively) and the specific heat $c_p$ are assumed to be independent of temperature; in this way the kinematic transport coefficients, i.e. $\nu = \mu/\rho$ and $\alpha = \lambda/\rho c_p$ (where $\rho$ is the fluid density) are directly proportional to the temperature. For the model problem, it is also assumed that the leading order pressure is constant in time as well as in space, conditions corresponding to an open system; even without this assumption, $p_0$ does not affect normal modes other than the zeroth one (which is not considered in the current analysis), since it is constant in space. These assumptions can be removed and are only made because the emphasis is in the presentation of the numerical scheme. A more general presentation of the numerical scheme is given in [14], whereas applications of this method to problems involving detailed transport and chemistry are given in [15, 16].

After nondimensionalization with appropriate reference quantities and incorporating all the above assumptions, the governing equations become

$$\frac{\partial T}{\partial t} + \mathbf{v}\cdot\nabla T = \frac{\alpha}{\mathrm{Re\,Pr}}\nabla^2 T + \dot{w}' \tag{1a}$$

$$1 = \rho T \tag{1b}$$

$$\frac{\partial \mathbf{v}}{\partial t} + \mathbf{v}\cdot\nabla\mathbf{v} = -\frac{1}{\rho}\nabla p_1 + \frac{\nu}{\mathrm{Re}}\left(\nabla^2\mathbf{v} + \frac{1}{3}\nabla(\nabla\cdot\mathbf{v})\right) \tag{1c}$$

$$\nabla\cdot\mathbf{v} = \frac{1}{\mathrm{Re\,Pr}}\nabla^2 T + \frac{\dot{w}'}{T}, \tag{1d}$$

where $\mathbf{v}$ is the velocity field, $T$ the temperature, $p_1$ is the first-order pressure or hydrodynamic pressure, and $\dot{w}'$ is the reaction term to be specified below. Here Re and Pr are the Reynolds and Prandtl numbers, respectively, and in their nondimensionalized form, $\alpha$ and $\nu$ are simply $\alpha = \nu = T$, since, as mentioned above, kinematic transport coefficients are directly proportional to the temperature; in addition, since the leading order pressure $p_0$ is constant in space and time, it is equal to 1 in nondimensional form. Equation (1d) replaces the mass conservation equation and has been obtained by combining the equations of energy, state, and continuity. It can be observed from Eq. (1d) that the only sources of nonzero divergence of the velocity field are the heat released by chemical reactions, and diffusive heat transfer (and for closed systems only, global compression or expansion).

## 2. LINEARIZED MODEL PROBLEM

The model problem described in this section was constructed in order to be used in the verification of the numerical approach outlined here and described in detail in [14]. As reported in [14], a purely 1D problem is not sufficient to assess the behavior of so-called "splitting errors" which are introduced because of the decoupling of the pressure and velocity calculations. Instead, a quasi 2D fixed boundary problem is developed from a 1D analytical solution of the conservation equations in a finite domain. The one-dimensional problem is the solution of the following system in the domain $x \in [-1, 1]$:

$$U_0\frac{\partial T_0}{\partial x} = \frac{\alpha}{\mathrm{Re\,Pr}}\frac{\partial^2 T_0}{\partial x^2} + \dot{w}'_0 \tag{2a}$$

$$U_0\frac{\partial U_0}{\partial x} = \frac{4\nu}{3\mathrm{Re}}\frac{\partial^2 U_0}{\partial x^2} - \frac{1}{\rho_0}\frac{\partial P_1}{\partial x} \tag{2b}$$

$$U_0\frac{\partial \rho_0}{\partial x} = -\rho_0\frac{\partial U_0}{\partial x} \tag{2c}$$

$$\rho_0 T_0 = 1, \tag{2d}$$

where $\nu = \alpha = T$. The reaction term in the energy equation is specified as

$$\dot{w}'_0 = \frac{1}{2\delta}\,\mathrm{sech}^2\left(\frac{x}{\delta}\right) + \frac{1}{\delta^2\,\mathrm{Re\,Pr}}\tanh\left(\frac{x}{\delta}\right)\mathrm{sech}^2\left(\frac{x}{\delta}\right), \tag{3}$$

where the parameter $\delta$ corresponds to the thickness of the temperature layer, as in Fig. 1.

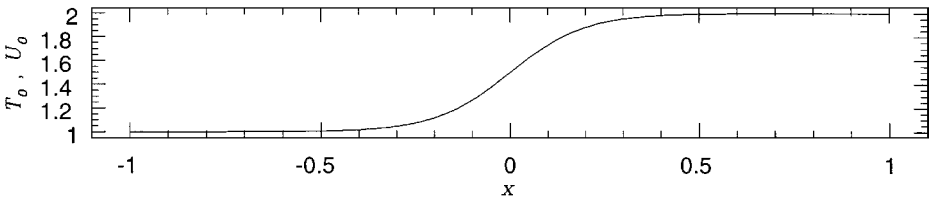


**FIG. 1.** Velocity $U_0$ and temperature $T_0$ for model problem.

The problem is closed by specifying boundary conditions to be

$$U_0(\pm 1) = T_0(\pm 1) = \frac{1}{2}\left(3 + \tanh\left(\frac{\pm 1}{\delta}\right)\right)$$

The solution of system (2a)–(2d) is simply

$$U_0(x) = T_0(x) = \frac{1}{2}\left(3 + \tanh\left(\frac{x}{\delta}\right)\right) \tag{4}$$

and the flow resembles a premixed flame located at $x = 0$ with reactants approaching the flame from the side $x = -1$, and products exiting the domain at $x = +1$. The reaction term (3) is chosen artificially to yield the flame front like solution (4). This form of the reaction term (3) does share some qualitative structure with that expected for premixed flames, but, due to the second term on the right side of (3), it has an artificial energy sink for $x < 0$ with $x \sim \delta$ and Re Pr $\leq \mathcal{O}(1)$.

The numerical solution of this 1D problem was performed using the numerical approach described in [14]. For the spatial discretization four spectral elements were used in the $x$ direction, and the number of collocation points inside each of these elements was varied from 5 to 15. This problem was solved as a time-dependent problem, i.e. with the time derivatives of $T_0, U_0$, and $\rho_0$ included in the left-hand sides of equations (2a), (2b), and (2c), respectively; the steady state solution to this problem is given by (4). It can be seen in Fig. 2 that the $L_2$ error of both the solution $U_0$ and of the divergence of the velocity field $dU_0/dx$ decay exponentially with respect to the number of collocation points. This kind of exponential decay of the error is typical of spectral type errors; however, for this problem the magnitude of the error is not affected by the time step $\Delta t$, but only by the spatial discretization error; i.e., the errors in Fig. 2 are almost independent of the value of $\Delta t$. The reason for this is that splitting errors are identically equal zero in 1D, and, the only source of error in the steady solution of system (2a)–(2d), is spatial discretization error. Therefore, in order to test all aspects of the numerical approach, a more complex model problem was constructed.

Following the analysis in [13], a linear stability analysis was performed for the one dimensional problem described by Eq. (4). The objective of this analysis is to obtain the least stable eigenmode with respect to perturbations in the transverse $y$-direction, which is assumed to be infinite in extent. Subsequently this least stable eigenmode is used as an initial condition for the time integrating scheme described in Section 3 and errors in the value of the decay rate (eigenvalue), and splitting errors are monitored during the integration. This new problem involving the integration of the two-dimensional linearized equations has all the required features to test the numerical scheme. The linearization around the base flow

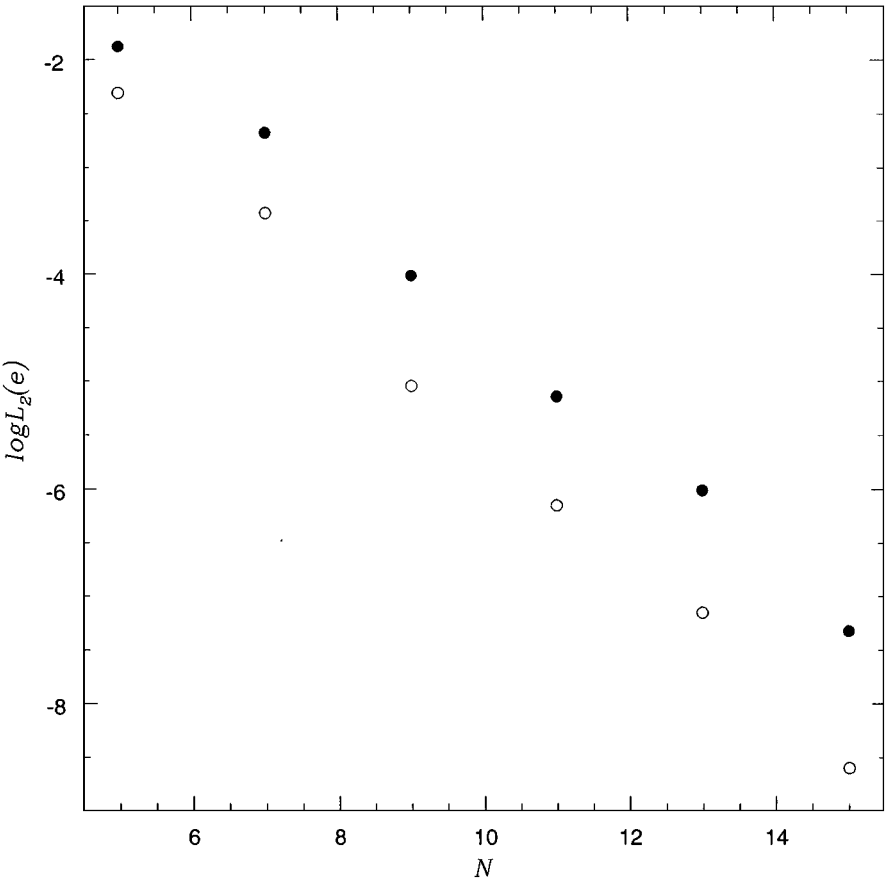


**FIG. 2.** Error $U_0 - U_{0,\text{exact}}$ and divergence error $\phi = \partial U_0/\partial x - (\partial U_0/\partial x)_{\text{exact}}$ as a function of number of collocation points for base flow of model problem.

$(T_0, U_0)$ is performed as

$$\begin{aligned} U(x,y,t) &= u'(x,y,t) + U_0(x) \\ V(x,y,t) &= v'(x,y,t) \\ P_1(x,y,t) &= p_1'(x,y,t) + P_1(x) \\ \rho(x,y,t) &= \rho'(x,y,t) + \rho_0(x) \\ T(x,y,t) &= T'(x,y,t) + T_0(x), \end{aligned} \tag{5}$$

where the primed quantities on the right side indicate the perturbation field. Substituting expressions (5) in the equations of motion (1a), (1c), and (1d) and keeping terms of first order in the perturbation quantities, the following linearized system of equations is obtained:

$$\frac{\partial u'}{\partial t} + U_0\frac{\partial u'}{\partial x} + u'\frac{dU_0}{dx} = \frac{T_0}{\text{Re}}\left(\frac{\partial^2 u'}{\partial x^2} + \frac{\partial^2 u'}{\partial y^2} + \frac{1}{3}\frac{\partial Q'}{\partial x}\right) - T_0\frac{\partial p_1'}{\partial x} + T'\frac{dU_0}{dx} \tag{6a}$$

$$\frac{\partial v'}{\partial t} + U_0\frac{\partial v'}{\partial x} = \frac{T_0}{\text{Re}}\left(\frac{\partial^2 v'}{\partial x^2} + \frac{\partial^2 v'}{\partial y^2} + \frac{1}{3}\frac{\partial Q'}{\partial y}\right) - T_0\frac{\partial p_1'}{\partial y} \tag{6b}$$

$$\frac{\partial T'}{\partial t} + U_0\frac{\partial T'}{\partial x} + u'\frac{dT_0}{dx} = \frac{T_0}{\mathrm{Re\,Pr}}\left(\frac{\partial^2 T'}{\partial x^2} + \frac{\partial^2 T'}{\partial y^2}\right) + \frac{T'}{\mathrm{Re\,Pr}}\frac{d^2T_0}{dx^2} \tag{6c}$$

$$Q' = \frac{\partial u'}{\partial x} + \frac{\partial v'}{\partial y} = \frac{1}{\mathrm{Re\,Pr}}\left(\frac{\partial^2 T'}{\partial x^2} + \frac{\partial^2 T'}{\partial y^2}\right) + \frac{T'}{T_0}\left(\frac{1}{\mathrm{Re\,Pr}}\frac{d^2T_0}{dx^2} - Q_0\right). \tag{6d}$$

In the derivation of these equations we have used Eq. (4), and the assumption that $\alpha = \nu = T$, whereas terms involving $1/\rho$ are linearized, to first order, as

$$\frac{1}{\rho} = \frac{1}{\rho_0}\left(1 - \frac{\rho'}{\rho_0}\right) = T_0\left(1 - \frac{\rho'}{\rho_0}\right).$$

This equation is the linearized form of the equation of state (1b). On the other hand, the reaction rate (3) is only a function of space, and not of the flow variables. Therefore, the reaction rate term does not contribute to the linearized equations. Equation (6d) again replaces the mass conservation equation and has been derived by combining the equations of energy, state, and continuity. The system (6a)–(6d) is a set of linear partial differential equations with variable coefficients, since the nonlinear terms have been linearized around the base solution $U_0$, $T_0$, and one can find normal mode solutions of this system if periodicity is assumed in the $y$ direction. The normal mode solutions are of the form

$$\begin{aligned} u'(x, y, t) &= Re\left[\hat{u}_k(x)\, e^{\sigma_k t}\, e^{iky}\right] \\ v'(x, y, t) &= Re\left[\hat{v}_k(x)\, e^{\sigma_k t}\, e^{iky}\right] \\ T'(x, y, t) &= Re\left[\hat{T}_k(x)\, e^{\sigma_k t}\, e^{iky}\right] \\ p_1(x, y, t) &= Re\left[\hat{p}_{1k}(x)\, e^{\sigma_k t}\, e^{iky}\right] \end{aligned} \tag{7}$$

Substituting (7) into (6a)–(6d), the following eigenvalue problem is obtained:

$$\sigma\hat{u}_k = -U_0\frac{\partial\hat{u}_k}{\partial x} - (\hat{u}_k + \hat{T}_k)\frac{dU_0}{dx} + \frac{T_0}{\mathrm{Re}}\left(\frac{\partial^2\hat{u}_k}{\partial x^2} - k^2\hat{u}_k + \frac{1}{3}\frac{\partial\hat{Q}_k}{\partial x}\right) - T_0\frac{\partial\hat{p}_{1k}}{\partial x} \tag{8a}$$

$$\sigma\hat{v}_k = -U_0\frac{\partial\hat{v}_k}{\partial x} + \frac{T_0}{\mathrm{Re}}\left(\frac{\partial^2\hat{v}_k}{\partial x^2} - k^2\hat{v}_k + \frac{ik\hat{Q}_k}{3}\right) - ikT_0\hat{p}_{1k} \tag{8b}$$

$$\sigma\hat{T}_k = -U_0\frac{\partial\hat{T}_k}{\partial x} + \hat{u}_k\frac{dT_0}{dx} + \frac{T_0}{\mathrm{Re\,Pr}}\left(\frac{\partial^2\hat{T}_k}{\partial x^2} - k^2\hat{T}_k\right) + \frac{\hat{T}_k}{\mathrm{Re\,Pr}}\frac{d^2T_0}{dx^2} \tag{8c}$$

$$\hat{Q}_k = \frac{\partial\hat{u}_k}{\partial x} + ik\hat{v}_k = \frac{1}{\mathrm{Re\,Pr}}\left(\frac{\partial^2\hat{T}_k}{\partial x^2} - k^2\hat{T}_k\right) + \frac{\hat{T}_k}{T_0}\left(\frac{1}{\mathrm{Re\,Pr}}\frac{d^2T_0}{dx^2} - Q_0\right) \tag{8d}$$

with boundary conditions $\hat{u}_k(x = \pm 1) = \hat{v}_k(x = \pm 1) = \hat{T}_k(x = \pm 1) = 0$. In order to calculate the leading eigenvalue $\sigma_k^*$ (with largest real part), an Arnoldi type method is used [17]. In this method, the largest eigenvalues are computable if we can evaluate $\mathbf{Lz}$ for various $\mathbf{z} = \{\hat{u}_k, \hat{v}_k, \hat{T}_k\}^{\mathrm{T}}$; we need not either evaluate $\mathbf{L}$ itself of $\mathbf{L}^{-1}$ or the like.

## 3. NUMERICAL SOLUTION OF MODEL PROBLEM

The integration of Eqs. (8a)–(8d) is performed using a mixed explicit–implicit splitting approach. For the numerical solution of this problem, the left-hand sides of Eqs. (8a), (8b), and (8c), are replaced by the time derivatives of $\hat{u}_k$, $\hat{v}_k$, and $\hat{T}_k$, respectively. In this way, the

numerically calculated decay rate of the least stable eigenmode, used as the initial condition to the mixed initial/boundary value problem, can be compared with its corresponding eigenvalue (true decay rate). The formal time integration method is based on backward differentiation and is the same scheme used to integrate the energy and species equations. A pressure Poisson equation, similar to that in incompressible flow, is derived for the hydrodynamic pressure $p_1$, accounting for the nonzero thermal divergence of the velocity field which is seen as a constraint enforced by the hydrodynamic pressure. In addition, although the right- and left-hand sides of (8d) have to be equal in the continuous (nondiscrete) form of the equations, in the following the divergence of the velocity field will be called $\hat{Q}_k = \partial \hat{u}_k/\partial x + ik\hat{v}_k$, whereas the right-hand side which is only a function of the temperature will be denoted as $\hat{Q}_{T,k}$. The difference between $\hat{Q}_k$ and $\hat{Q}_{T,k}$ will be used as a measure of the error caused by the splitting.

The integration of the momentum equation (8a)–(8b) is explicit for the linearized convective terms, whereas it is implicit for the viscous and pressure terms, as in

$$\sum_{q=0}^{J-1} \frac{\alpha_q \hat{u}_k^{n+1-q}}{\Delta t} = -\sum_{q=0}^{J-1} \beta_q \left( U_0 \frac{\partial \hat{u}_k}{\partial x} + \hat{u}_k \frac{dU_0}{dx} \right)^{n-q} + \frac{T_0}{\mathrm{Re}} \left( \frac{\partial^2 \hat{u}_k}{\partial x^2} - k^2 \hat{u}_k + \frac{1}{3} \frac{\partial \hat{Q}_{T,k}}{\partial x} \right)^{n+1} - T_0 \frac{\partial \hat{p}_{1k}}{\partial x} + \hat{T}_k^{n+1} \frac{dU_0}{dx} \tag{9a}$$

$$\sum_{q=0}^{J-1} \frac{\alpha_q \hat{v}_k^{n+1-q}}{\Delta t} = -\sum_{q=0}^{J-1} \beta_q U_0 \frac{\partial \hat{v}_k^{n-q}}{\partial x} - ikT_0 \hat{p}_{1k} + \frac{T_0}{\mathrm{Re}} \left( \frac{\partial^2 \hat{v}_k}{\partial x^2} - k^2 \hat{v}_k + \frac{ik\hat{Q}_{T,k}}{3} \right)^{n+1} \tag{9b}$$

$$\sum_{q=0}^{J-1} \frac{\alpha_q \hat{T}_k^{n+1-q}}{\Delta t} = -\sum_{q=0}^{J-1} \beta_q \left( U_0 \frac{\partial \hat{T}_k}{\partial x} + \hat{u}_k \frac{dT_0}{dx} \right)^{n-q} + \frac{T_0}{\mathrm{Re\,Pr}} \left( \frac{\partial^2 \hat{T}_k}{\partial x^2} - k^2 \hat{T}_k + \frac{\hat{T}_k}{T_0} \frac{d^2 T_0}{dx^2} \right)^{n+1} \tag{9c}$$

$$\hat{Q}_{T,k}^{n+1} = \frac{1}{\mathrm{Re\,Pr}} \left( \frac{\partial^2 \hat{T}_k}{\partial x^2} - k^2 \hat{T}_k \right)^{n+1} + \frac{\hat{T}_k^{n+1}}{T_0} \left( \frac{1}{\mathrm{Re\,Pr}} \frac{d^2 T_0}{dx^2} - Q_0 \right). \tag{9d}$$

The pressure Poisson equation is derived by taking the divergence of the linearized momentum equations (9a)–(9b) as

$$\begin{aligned} \frac{\partial}{\partial x} \left( T_0 \frac{\partial \hat{p}_{1k}}{\partial x} \right) - k^2 T_0 \hat{p}_{1k} = & -\frac{\sum_{q=0}^{J-1} \alpha_q \hat{Q}_k^{n+1-q}}{\Delta t} - ikU_0 \sum_{q=0}^{J-1} \beta_q \frac{\partial \hat{v}_k^{n-q}}{\partial x} \\ & - \frac{\partial}{\partial x} \left( \sum_{q=0}^{J-1} \beta_q \left( U_0 \frac{\partial \hat{u}_k}{\partial x} + \hat{u}_k \frac{dU_0}{dx} \right)^{n-q} + \hat{T}_k^{n+1} \frac{dU_0}{dx} \right) \\ & + \frac{\partial}{\partial x} \frac{T_0}{\mathrm{Re}} \left( \frac{4}{3} \frac{\partial \hat{Q}_{T,k}^{n+1}}{\partial x} - ik \sum_{q=0}^{J-1} \beta_q \hat{\omega}_k^{n-q} \right) \\ & + ik \frac{T_0}{\mathrm{Re}} \left( \frac{4}{3} ik \hat{Q}_{T,k}^{n+1} + \sum_{q=0}^{J-1} \beta_q \frac{\partial \hat{\omega}_k^{n-q}}{\partial x} \right), \end{aligned} \tag{9e}$$

where $\hat{\omega}_k$ is the vorticity which is equal to $\hat{\omega}_k = \partial \hat{v}_k/\partial x - ik\hat{u}_k$. It has to be noted that

pressure $\hat{p}_{1k}$ is not governed by a predictive equation (i.e., no term $\partial \hat{p}_{1k}/\partial t$ appears in any of the equations above) and is in equilibrium with the velocity field at each time step. Therefore, it does not really require a superscript $n+1$. The right-hand side of the pressure equation (9e) does not contain the velocity at the new time level $t^{n+1}$. In order to decouple the pressure and velocity calculation, these terms involving $\{\hat{u}_k, \hat{v}_k\}^{n+1}$ in the pressure equation have been expressed in terms of known quantities. This was performed using the identities

$$\frac{\partial^2 \hat{u}_k}{\partial x^2} - k^2 \hat{u}_k = \frac{\partial}{\partial x}\left(\frac{\partial \hat{u}_k}{\partial x} + ik\hat{v}_k\right) - ik\left(\frac{\partial \hat{v}_k}{\partial x} - ik\hat{u}_k\right) \tag{10a}$$

$$\frac{\partial^2 \hat{v}_k}{\partial x^2} - k^2 \hat{v}_k = ik\left(\frac{\partial \hat{u}_k}{\partial x} + ik\hat{v}_k\right) + \frac{\partial}{\partial x}\left(\frac{\partial \hat{v}_k}{\partial x} - ik\hat{u}_k\right) \tag{10b}$$

and by using the irrotational-solenoidal decomposition of the velocity field $\mathbf{v}_k = \mathbf{v}_{k,S} + \mathbf{v}_{k,I}$ (where $\mathbf{v}_k = \{\hat{u}_k, \hat{v}_k\}$) and treating the terms involving $\mathbf{v}_{k,I}$ implicitly (using the known "thermal" divergence of the velocity field $\hat{Q}_{T,k}^{n+1}$) as

$$\hat{Q}_k^{n+1} = \left(\frac{\partial \hat{u}_k}{\partial x} + ik\hat{v}_k\right)^{n+1} = \left(\frac{\partial \hat{u}_k}{\partial x} + ik\hat{v}_k\right)_I^{n+1} \approx \hat{Q}_{T,k}^{n+1}.$$

The same substitution has been used for the implicit calculation of the viscous terms when solving for the new velocity components $\{\hat{u}_k, \hat{v}_k\}^{n+1}$ in Eqs. (9a)–(9b). Substituting $\hat{Q}_{T,k}^{n+1}$ for $\hat{Q}_k^{n+1}$ in the equations above is only done to decouple the pressure and velocity calculation, and it does not mean that the difference between $\hat{Q}_{T,k}^{n+1}$ and $\hat{Q}_k^{n+1}$ will be equal to zero at the end of each time step. In fact, it is this difference that governs splitting errors, which are analyzed in Section 4. For the solenoidal part, an explicit extrapolation is used, resulting in

$$\hat{\omega}_k^{n+1} = \left(\frac{\partial \hat{v}_k}{\partial x} - ik\hat{u}_k\right)^{n+1} = \left(\frac{\partial \hat{v}_k}{\partial x} - ik\hat{u}_k\right)_S^{n+1} \approx \sum_{q=0}^{J-1} \beta_q \hat{\omega}_k^{n-q}.$$

This procedure is similar to methods used in splitting methods for incompressible flows (see [13, 18]). The boundary conditions used for the pressure equation are derived by taking the dot product of Eqs. (6a)–(6b) in the direction normal to the boundaries $\mathbf{n}$ (in this case simply $x$) and making the substitutions mentioned above. In this way, a Neumann pressure boundary condition is obtained for Dirichlet velocity boundaries, namely,

$$\frac{\partial \hat{p}_{1k}}{\partial x} = \frac{1}{\mathrm{Re}}\left(\frac{4}{3}\frac{\partial \hat{Q}_{T,k}^{n+1}}{\partial x} - ik\sum_{q=0}^{J-1} \beta_q \hat{\omega}_k^{n-q}\right). \tag{11}$$

In summary, the solution method proceeds as follows: The energy equation is solved independently since the convective terms, which couple the energy and momentum equations, are calculated explicitly. The splitting scheme for the momentum equations involves first calculating the explicit convective terms and then solving for the pressure from Eqs. (9e), and (11); subsequently, the incorporation of the pressure correction to the velocity field is performed, followed by the integration of the viscous part of the momentum equation which is performed implicitly. The boundary conditions for the velocity are incorporated in the viscous step as well. The solution procedure is then completed by choosing a method for the spatial discretization. The methods used in this work are either global spectral methods or spectral element methods, which are described extensively in [19–22].

In the following section, it will be demonstrated that the splitting procedure described in this section gives overall high-order accuracy in time and minimal errors in mass conservation, or so-called splitting errors. The behavior of these errors is obtained using an approximate asymptotic analysis. It is shown that splitting errors are always smaller than the formal truncation error $\mathcal{O}(\Delta t^J)$ of the $J$th-order integrating scheme.

## 4. ERROR IN MASS CONSERVATION DUE TO SPLITTING

In order to obtain an estimate for splitting errors, an equation for the difference between the divergence of the velocity field $\hat{Q}_k^{n+1}$ and the "thermal" divergence $\hat{Q}_{T,k}^{n+1}$ has to be obtained. The "thermal" divergence $\hat{Q}_{T,k}^{n+1}$ is viewed as a constraint on the velocity field, the same way that condition $\hat{Q}_k^{n+1} = 0$ is a constraint for incompressible flow. In order to derive an equation for the difference $\phi = \hat{Q}_k^{n+1} - \hat{Q}_{T,k}^{n+1}$, we combine the divergence of Eqs. (9a) and (9b) and Eq. (9e) to obtain

$$\left(\frac{\gamma_0}{\Delta t} + \frac{k^2}{\mathrm{Re}}\right)\phi - \frac{1}{\mathrm{Re}}\frac{\partial}{\partial x}T_0\frac{\partial \phi}{\partial x} = ik\frac{\partial T_0}{\partial x}\left(\hat{\omega}_k^{n+1} - \sum_{q=0}^{J-1}\beta_q\hat{\omega}_k^{n-q}\right). \tag{12}$$

This is an elliptic (variable coefficient Helmholtz) equation for the difference $\phi = \hat{Q}_k^{n+1} - \hat{Q}_{T,k}^{n+1}$, between the divergence at time step $t^{n+1}$ and the value dictated by the energy equation from Eq. (9d). It was mentioned in the beginning of Section 2 that a purely 1D problem is not sufficient to assess the behavior of splitting errors. Although Eq. (12) is one-dimensional, it is the result of the two-dimensional linear stability analysis, described in 3, and has all required features to test the numerical scheme. For example, the same equation for a purely 1D problem is homogeneous, since in that case, the only relevant wavenumber would be $k = 0$. The right-hand side of this elliptic equation is nonzero only when the viscosity is variable, i.e. when $T_0$ is not constant. For a general nonlinear problem, this viscosity is not only a function of the base temperature $T_0$, but of the total temperature and the species concentrations as well; its simple form here is only a result of linearization. In addition, the right-hand side of (12) is of order $\mathcal{O}(\Delta t^J)$, where $J$ is the order of the time stepping used (typically up to $J = 3$), and its maximum is $\mathcal{O}(\Delta t)$. To find the boundary condition for (12), Eqs. (11) and (9a) are combined to obtain

$$\frac{4}{3}\frac{\partial \phi}{\partial x} = -ik\left(\sum_{q=0}^{J-1}\beta_q\hat{\omega}_k^{n-q} - \hat{\omega}_k^{n+1}\right). \tag{13}$$

Both Eq. (12) for $\phi$ and its boundary condition (13) have a nonhomogeneous part which scales with $\mathcal{O}(\Delta t^J)$. The nonzero boundary condition (13) is the cause of splitting errors that also appear in incompressible flows (homogeneous solution), whereas the nonzero right-hand side of Eq. (12) is the part of the error which is caused by the compressibility, and only when the kinematic viscosity is spatially varying.

In this section, the error in mass conservation due to splitting will be analyzed for the case of small values of $\Delta t/\mathrm{Re}$. A one-dimensional problem, which incorporates most of the important features of the problem, is used for the asymptotic study. It is assumed that the temperature $T$ varies in layers of thickness much larger than the length scale $(\Delta t/\mathrm{Re})^{1/2}$. This means that if the temperature has a local structure somewhere similar to $\tanh(x/\delta)$,

typical of flame fronts, then the length scale $\delta \gg (\Delta t/\mathrm{Re})^{1/2}$. The domain of interest extends from $x=-1$ to $x=+1$, and the boundary conditions are derived from (12). Equation (12) becomes

$$\varepsilon^2\phi'' + \varepsilon^2 a(x)\phi' + b(x)\left(\gamma_0 + \varepsilon^2 k^2\right)\phi = \varepsilon^2 a(x)\Delta\omega_s, \tag{14}$$

whereas the boundary conditions are

$$\phi'(\pm 1) = \frac{3}{4}\Delta\omega_s|_{\pm 1}. \tag{15}$$

Here $\phi = \hat{Q}_k^{n+1} - \hat{Q}_{T,k}^{n+1}$, $\Delta\omega_s = ik(\hat{\omega}_k^{n+1} - \sum_{q=0}^{J-1}\beta_q\hat{\omega}_k^{n-q})$, and $\varepsilon = (\Delta t/\mathrm{Re})^{1/2}$. Because $\hat{\omega}_k$ has the opposite parity of $\hat{Q}_k$, the right side of Eq. (14) has the same parity with the left side. The functions $a(x)$ and $b(x)$ are given by $a(x) = T_0'/T_0$ and $b(x) = -1/T_0$. It will be assumed later that $\Delta\omega_s$ is of order $\Delta t^J$ everywhere, for $J$th-order time stepping, in order to get global estimates for $\phi$. Equation (14) is a nonhomogeneous singularly perturbed ordinary differential equation. The problem is divided into two separate problems, one with nonzero right-hand side and zero boundary conditions (the particular solution $\phi_P$, corresponding to

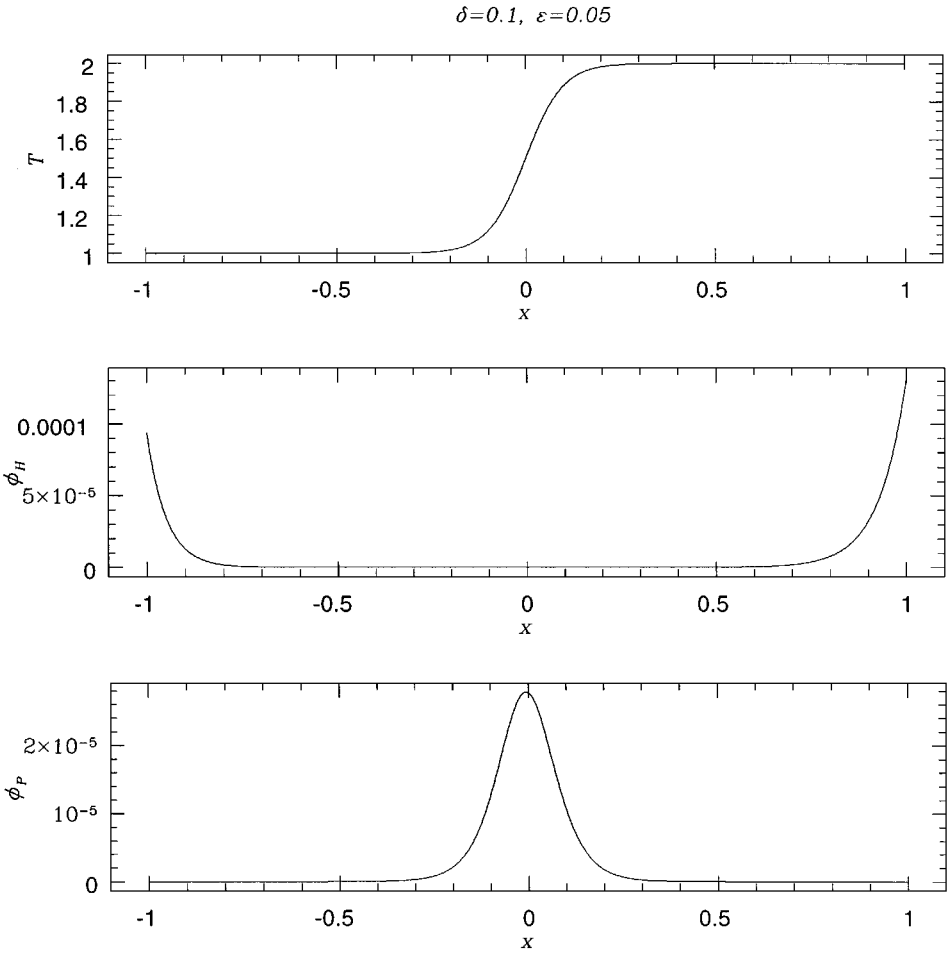


**FIG. 3.** Distribution of temperature and divergence error for $\varepsilon = 0.05$, $\delta = 0.1$, and $\Delta\omega_s = \varepsilon^2$.

errors because of compressibility), and one with zero right-hand side and nonzero boundary conditions (the homogeneous solution $\phi_H$, corresponding to standard splitting errors). A particular solution to this equation is found by first constructing the Green's function of the differential operator of Eq. (14) using the WKB method and then finding the particular solution of the nonhomogeneous problem. Using WKB, it is found that the general solution has the form to $\mathcal{O}(\varepsilon)$

$$\phi(x) = A_{\pm} T^{-1/4} \exp\left(\pm \frac{1}{\varepsilon} \int^{x} \frac{dt}{T^{1/2}(t)}\right), \tag{16}$$

where $A_{\pm}$ are constants determined by the boundary conditions. The solutions $\phi_P$ and $\phi_H$ are found, to leading order, to be

$$\phi_P(x) = \varepsilon^2 \Delta\omega_s T'(x) + \mathcal{O}\left(\varepsilon^4 \Delta\omega_s\right) \tag{17}$$

$$\phi_H(x) = \tfrac{3}{4} \varepsilon \Delta\omega_s|_{\pm 1} T^{-1/4}(x) f(x) + \mathcal{O}\left(\varepsilon^2 \Delta\omega_s|_{\pm 1}\right). \tag{18}$$

This means that if the quantity $\Delta\omega_s$ is globally of order $\Delta t$ or $\varepsilon^2$Re (for a first-order overall scheme), the overall error in the interior of the domain, because of the inhomogeneity of (14), is $\mathcal{O}(\Delta t^2/\mathrm{Re})$. Similarly the error in the interior for a time integration scheme of order

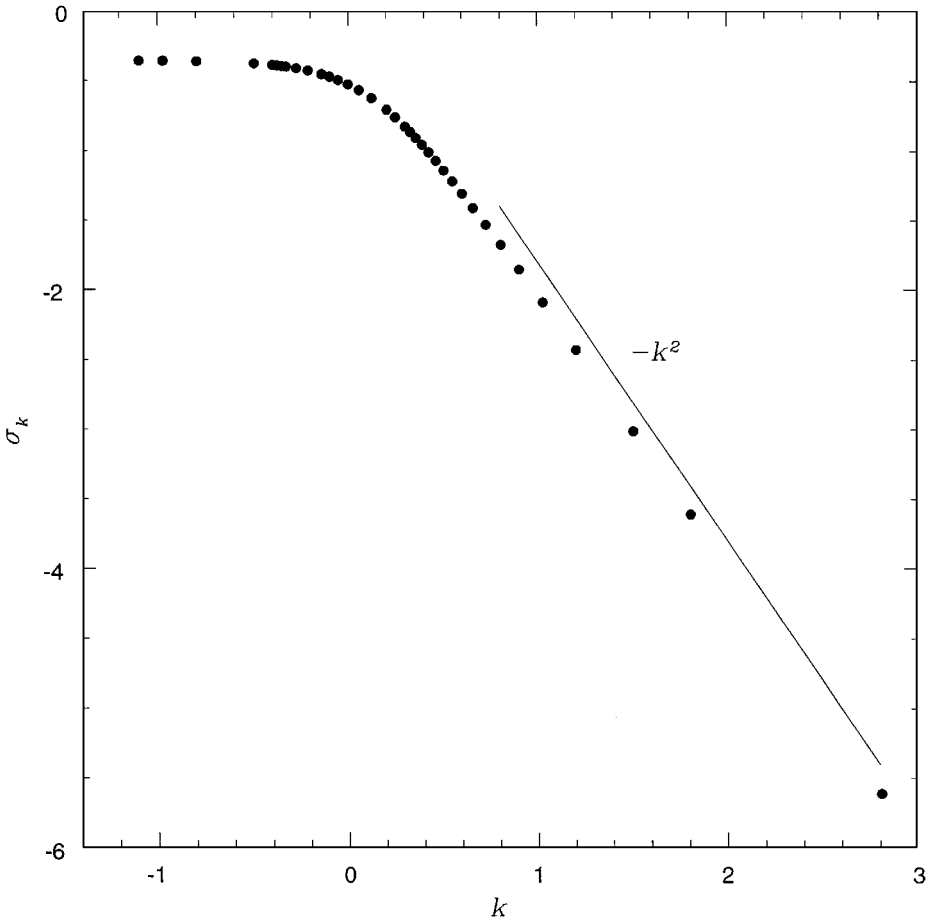


**FIG. 4.** Distribution of eigenvalues $\sigma_k$ for the linear stability problem with $\delta = 0.2$.

$J$ would be $\mathcal{O}(\Delta t^{J+1}/\mathrm{Re})$. For simplicity we have assumed that $\Delta\omega_s(-1) = \Delta\omega_s(+1)$. On the other hand, again assuming that $\Delta\omega_s(\pm 1)$ is $\mathcal{O}(\varepsilon^2\,\mathrm{Re})$, the error close to the domain boundaries, which is the effect of nonhomogeneous boundary conditions, becomes $\mathcal{O}(\Delta t^{3/2}/\mathrm{Re}^{1/2})$. This estimate is true in boundary layers of $\mathcal{O}(\varepsilon)$ close to the boundaries $x \sim \pm(1-\varepsilon)$, where the function $f(x)$ gives an overall contribution of $\mathcal{O}(1)$. In the rest of the domain, the function $f(x)$ in (18) is exponentially small. Therefore, the error in mass conservation is $\mathcal{O}(\Delta t^{J+1/2}/\mathrm{Re}^{1/2})$ in boundary layers of $\mathcal{O}(\varepsilon)$ away from the boundaries, whereas it is $\mathcal{O}(\Delta t^{J+1}/\mathrm{Re})$ in the interior of the domain for a general $J$th-order time integration scheme.

In Fig. 3, we plot the distribution of the two sources of divergence error, from the nonzero inhomogeneity and the nonzero boundary condition respectively. The case plotted is for $\varepsilon = 0.05$, $\delta = 0.1$, and $\Delta\omega_s = \varepsilon^2$, and corresponds to the temperature profile, $T = 0.5(3 + \tanh(x/\delta))$, shown in Fig. 1.

## 5. NUMERICAL RESULTS

The eigenspectrum of (8a)–(8d) for different values of the $y$-wavenumber $k$ is calculated using the numerical approach described at the end of Section 2 for the case $\delta = 0.2$ and $\mathrm{Re} = \mathrm{Pr} = 1$. The least stable eigenvalues $\sigma_k^*$ of this system are plotted in Fig. 4 as a function

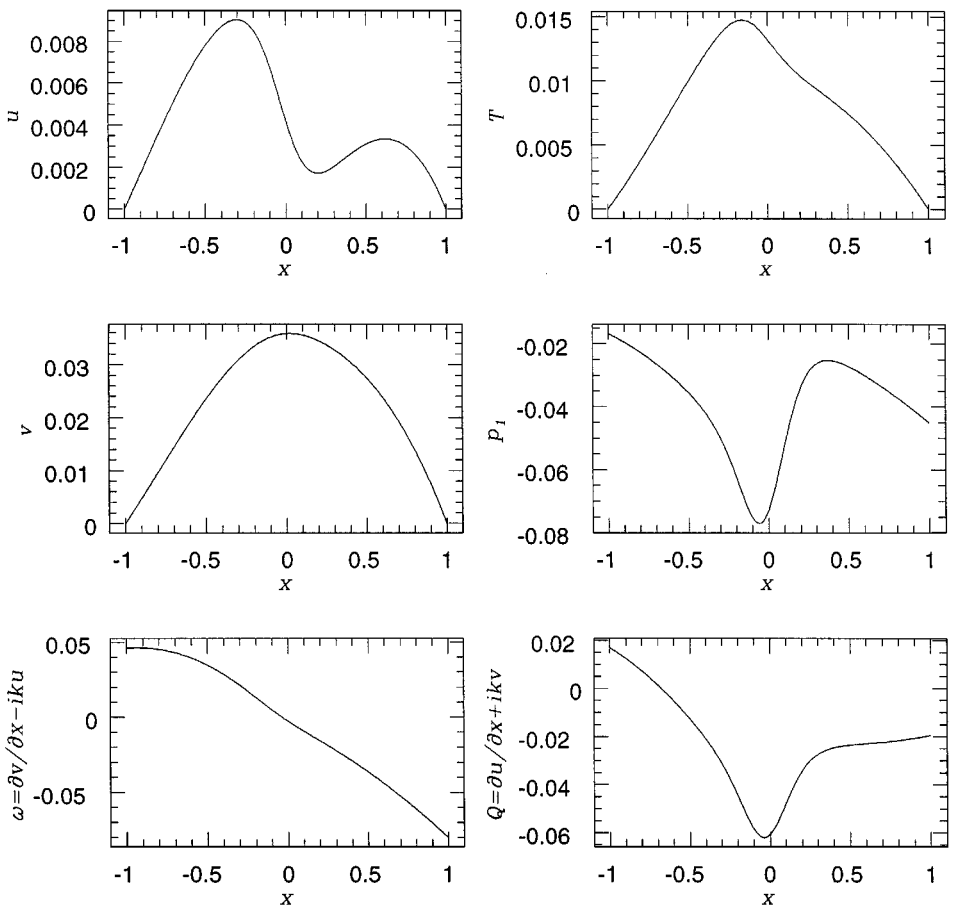


**FIG. 5.** Least stable eigenvector for $k = 1$, $\delta = 0.2$, and $\mathrm{Re} = \mathrm{Pr} = 1$.

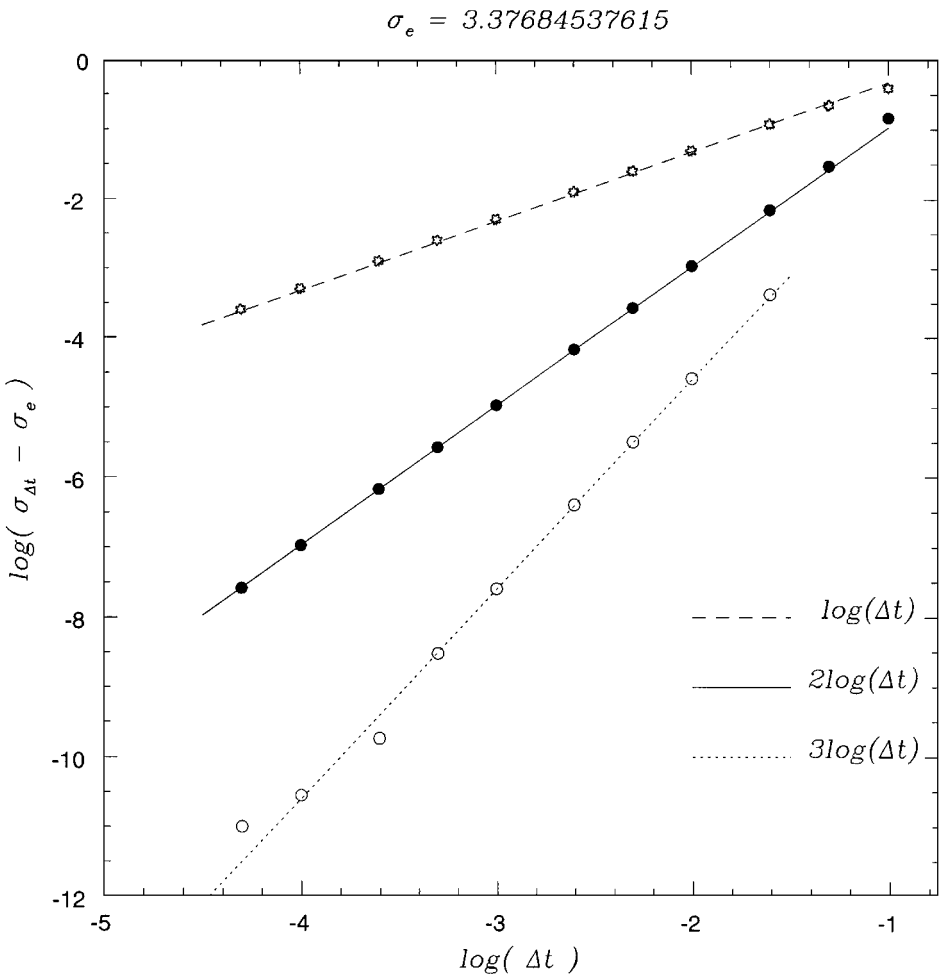


**FIG. 6.** Error in decay rate $\sigma_e$ using different order integrating schemes.

of $k$. As can be observed from the figure for high values of the wavenumber $k$ the spectrum behaves like $-k^2$ as expected, since small scales are viscously damped.

The least stable eigenvector for $k = 1$ corresponding to the leading eigenvalue of $\sigma_1^* = -3.37684537615$ is plotted in Fig. 5. This eigenvector was subsequently used as an initial condition for the solution of system (9a)–(9e) as an initial-boundary value problem using the numerical approach described in Section 3.

In Fig. 6, the error in the value of the decay rate, as obtained by a time-dependent simulation of the linearized two-dimensional problem, using first, second, and third order time integrating schemes, is shown. As can be observed from this figure, first, second, and third order accuracy is obtained, respectively, for each of the schemes used, which demonstrates the fact that splitting errors are of higher order and do not destroy the formal order of accuracy. The spatial resolution used in these simulations was 257 Legendre collocation points in the $x$-direction.

In addition, the value of the error in mass conservation is plotted as function of $\Delta t$ in Figs. 7a and 7b. The divergence errors at the domain boundary (a) and at the middle of the domain (b) are indicated as symbols in these plots for different time stepping orders and values of $\Delta t$; also shown as lines in these plots are the asymptotic estimates obtained

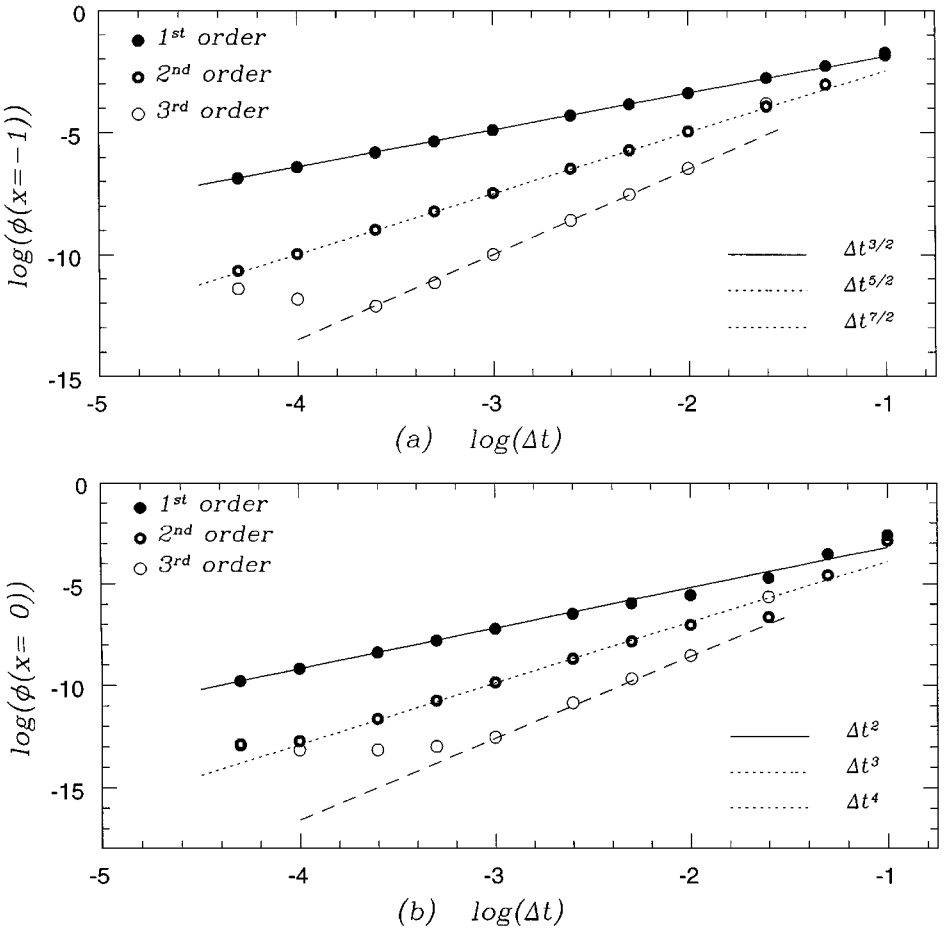


**FIG. 7.** Distribution of mass conservation errors at (a) $x = -1$ and (b) $x = 0$, respectively, for *first*, *second*, and *third* order, respectively.

in Section 4. As can be observed, when the value of $\varepsilon = (\Delta t/\mathrm{Re})^{1/2}$ is small enough with respect to the "flame thickness" (here $\delta = 0.2$), i.e. when $\Delta t \leq 0.01$ (for $\mathrm{Re} = \mathrm{Pr} = 1$), the results of the asymptotic analysis agree well with the smulations. Also, for very low values of $\Delta t$ the errors for the third-order scheme are very close to the spatial discretization errors (which for 257 Legendre points leads to a spatial error of $\mathcal{O}(10^{-12})$), saturating at roundoff error. Therefore, the estimates obtained for the behavior of splitting errors and the overall accuracy of the numerical scheme are fairly reliable.

## 6. CONCLUSIONS

In this work, we have presented and analyzed a quasi-two-dimensional model problem, which can be used as a benchmark problem for verification of numerical methods for the solution of low speed compressible reactive flow problems with applications in combustion. Since an expansion in terms of normal modes is used in one direction ($y$), the computational cost associated with the solution of this problem is essentially the same as the cost of a 1D problem. This model problem was constructed because of the need to analyze a new

numerical approach for the low Mach number equations and to quantify its error behavior in a nontrivial case; the sensitivity of the decay rate of the least stable eigenmode of the model problem to small perturbations provides a challenging test-case for numerical algorithms. Moreover, the solution of this quasi-two-dimensional problem provides information on the spatial distribution of errors and, in particular, of splitting errors and allows for the evaluation of the overall convergence rate of the methods used.

Numerical experiments based on the model problem were performed and were used for the testing of a recently developed numerical approach for these types of problems; numerical results were compared with asymptotic estimates for the behavior of splitting errors and were found to be in agreement. Splitting errors were found to be smaller than the formal truncation errors of the integrating scheme; moreover, our numerical approach leads to overall high order accuracy in time with minimal errors in mass conservation as well as to a partially decoupled solution procedure. The benchmark problem presented here can be used by other researchers for detailed analysis of the error behavior of other numerical methods.

This work was supported by ARPA/ONR URI Grant N00014-92-J-1796. Part of this work was completed while the first author was at the Institute of Energy Technology/LVV of the Swiss Federal Institute of Technology, Zurich (ETHZ), Switzerland.

## REFERENCES

1. B. T. Chu and L. S. G. Kovasznay, Non-linear interactions in a viscous heat-conducting compressible gas, *J. Fluid Mech.* **3**, 494 (1958).
2. G. J. Sivashinsky, Hydrodynamics theory of flame propagation in an enclosed volume, *Acta Astronaut.* **6**, 631 (1979).
3. G. R. Rehm and H. R. Baum, The equations of motion for thermally driven flows, *J. Res. Natl. Bur. Standards* **83**(3), 297 (1978).
4. E. S. Oran and J. P. Boris, *Numerical Simulation of Reactive Flow* (Elsevier Science, New York, 1987).
5. M. Smooke, R. Mitchell, and D. Keyes, Numerical solution of two-dimensional axisymmetric laminar diffusion flames, *Combust. Sci. Technol.* **67**, 85 (1989).
6. T. Poinsot, S. Candel, and A. Trouvé, Applications of direct numerical simulation to premixed turbulent combustion, *Prog. Energy Combust. Sci.* **21**, 531 (1996).
7. P. A. McMurtry, W. H. Jou, J. J. Riley, and R. W. Metcalfe, Direct numerical simulations of a reacting mixing layer with chemical heat release, *AIAA J.* **24**(6), 962 (1986).
8. R. I. Issa, B. Ahmadi-Befrui, K. R. Beshay, and A. D. Gosman, Solution of the implicitly discretised reacting flow equations by operator-splitting, *J. Comput. Phys.* **93**(2), 388 (1991).
9. J. Hilditch and P. Colella, A projection method for low Mach number fast chemistry reacting flow, in *AIAA Aerospace Sciences Meeting, Jan. 6–10, Reno, NV., 1997.*
10. S. Lele, Compact finite difference schemes with spectral like resolution, *J. Comput. Phys.* **103**, 16 (1992).
11. T. Poinsot and S. Lele, Boundary conditions for direct simulations of compressible viscous flows, *J. Comput. Phys.* **101**, 104 (1992).
12. N. Yanenko, *The Method of Fractional Steps* (Springer-Verlag, Berlin, New York, 1971).
13. S. A. Orszag, M. Israeli, and M. O. Deville, Boundary conditions for incompressible flows, *J. Sci. Comput.* **1**, 75 (1986).
14. A. G. Tomboulides, J. Lee, and S. A. Orszag, Numerical simulation of low mach number reactive flows, *J. Sci. Comput.* **12**, 139 (1997).
15. J. Lee, A. G. Tomboulides, S. A. Orszag, R. Yetter, and F. Dryer, A transient two-dimensional chemically reactive flow model: Fuel particle combustion in a non-quiescent environment, in *Twenty-sixth Symposium(International) on Combustion/The Combustion Institute, 1996.*

16. J. Lee, *Simulations of Two-Dimensional Chemically Reactive Flows*, Ph.D. thesis, Princeton University, 1996.
17. M. Israeli and A. Sidi, personal communication, Arnoldi-type eigensolvers provided.
18. G. E. Karniadakis, M. Israeli, and S. A. Orszag, High-order splitting methods for the incompressible Navier–Stokes equations, *J. Comput. Phys.* **97**, 414 (1991).
19. D. Gottlieb, and S. A. Orszag, *Numerical Analysis of Spectral Methods: Theory and Applications* (SIAM, Philadelphia, 1977).
20. C. Canuto, M. Hussaini, A. Quarteroni, and T. Zang, *Spectral Methods in Fluid Dynamics* (Springer-Verlag, New York/Berlin, 1987).
21. A. T. Patera, A spectral element method for fluid dynamics; Laminar flow in a channel expansion, *J. Comput. Phys.* **54**, 468 (1984).
22. Y. Maday and A. T. Patera, Spectral element methods for the Navier–Stokes equations, in *ASME, State-of-the-Art Surveys in Computational Mechanics, 1987*.